https://doi.org/10.15407/ufm.20.04.620

Z.M. RYKAVETS [1], J. BOUQUEREL [2], J.-B. VOGT [2], Z.A. DURIAGINA [1,3], V.V. KULYK [1], T.L. TEPLA [1], L.I. BOHUN [1], and T.M. KOVBASYUK [1]

[1] Lviv Polytechnic National University,
12 Bandera Str., UA-79013 Lviv, Ukraine
[2] The Lille 1 University of Science and Technology,
Unité Matériaux et Transformations,
Cité Scientifique, F-59650 Villeneuve-d'Ascq, France
[3] John Paul II Catholic University of Lublin,
14 Al. Racławickie, PL-20-950 Lublin, Poland

INVESTIGATION OF THE MICROSTRUCTURE AND PROPERTIES OF TRIP 800 STEEL SUBJECTED TO LOW-CYCLE FATIGUE

Low-alloyed TRIP steels are well known since the beginning of the 21st century and used for automotive applications to ensure the passive safety. However, although their behaviour is fully investigated at a monotonous behaviour, the case of cyclic loading is not well studied. The present work describes in detail the heterogeneous-microstructure evolution of a high-strength steel (TRIP 800 steel) at the low-cycle fatigue conditions. Based on the extended investigations (*via* the optical and electron microscopy, the electron backscattering diffraction), we propose suggestions on the influence of phase composition on the mechanical properties and the crack-initiation processes. The preferential places of the crack nucleation caused by fatigue are detected, and the completeness of phase transformation *via* the induced plasticity is evaluated.

Keywords: low-cycle fatigue, microstructure, fractography, electron backscatter diffraction.

1. Introduction

Within the last decades, a considerable attention has been paid to the Transformation Induced Plasticity effect occurring in steels containing metastable austenite. In addition, a special category of advanced high strength steels (AHSS), called low-alloyed TRIP aided steels, has been

developed in order to be used by the automotive industry for the body in white (BIW) vehicle structure. The properties of such steels are remarkable as they exhibit a great combination of mechanical strength and ductility. Such a combination is directly linked to both the synergy of the different constituting phases and the ability of the retained austenite to transform to martensite when the steel is submitted to mechanical loading. It should be noted that similar phenomena of structuring occur during the use of high-energy surface engineering methods [1, 2]. As those steels possess an enhanced formability and a high dynamic energy absorption during high strain rate crash deformation (350 $MJ \cdot m^{-3}$ at 1000 s^{-1}) [3] , it makes them suitable for automotive industry [4–6], promoting safety and BIW design.

Moreover, as this kind of steel can be used for lightweight vehicle structural components, its fatigue behaviour might be investigated. Indeed, acquire the knowledge on the behaviour of TRIP steel submitted to low or high cycle fatigue may prevent from in-use accidents.

Low alloyed TRIP steels are known to own a multiphase structure and contain ferrite (50–60%), carbide free bainite (B) and carbon enriched retained austenite (A) (10–20%). Some investigations also report that part of this metastable austenite might already transformed, which leads to the presence of a martensite/austenite constituent (M/A) [7]. In addition, to ensure the TRIP effect, the grain size of the retained austenite (γ) must be in 0.01μm to 1μm range [8]. Moreover, the stability of retained austenite is stress state dependent *i.e.* the highest [3] for uniaxial compression and the lowest for plane strain conditions. If retained austenite is unstable, it transforms to martensite early during deformation without any sensitive effect on ductility regardless of its amount [6]. During plastic deformation, the transformation of retained austenite to martensite provided a localized work-hardening effect which relaxed the stress concentration, delaying the onset of necking, and, increasing the uniform elongation. The newly formed hard martensite phase enhanced tensile strength [9, 10].

Although the behaviour of TRIP steels is well studied for monotonic deformation (as encountered for the sheet steel forming) and dynamic situation (as encountered for crash conditions), studies focusing on the mechanical properties of TRIP steels when those latter are submitted to cyclic loading are quite recent [11–16]. Nevertheless, a few attentions have been paid to the microstructure evolution and its influence on fatigue crack initiation or propagation [13], so that the link between the microstructure evolution and the obtained mechanical properties remains unclear. In the present work, a TRIP 800 steel has been submitted to cyclic loadings and its microstructure evolution has been investigated by means of standard metallurgical investigations as well as advanced analysis by EBSD.

2. Experimental Procedure

2.1. Material

The material of the study is a low alloyed CMnSi TRIP aided steel with the chemical composition given in Table 1. The material has been provided in thin sheet of 1 mm in thickness, but the supplier has given no details regarding the rolling conditions. Nevertheless, when referring to literature, it is supposed to be obtained by a standard TRIP steel thermomechanical processing, which consists of the following steps as represented in Fig. 1.

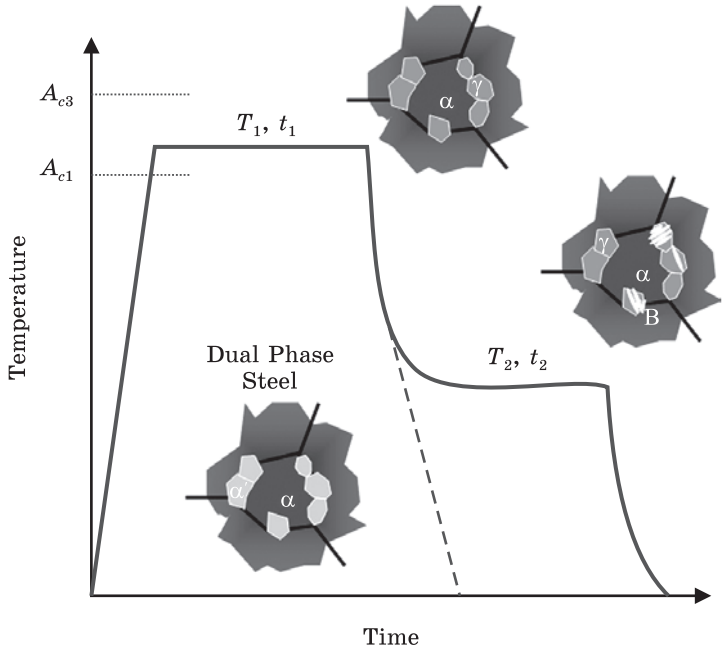

Fig. 1. Typical two step processing route (in terms of temperature, T, and time, t) leading to the TRIP steel microstructure for low-alloyed carbon steel (α — ferrite, γ — austenite, B — bainite, α′ — martensite)

Table 1. **Chemical composition of the studied TRIP 800 steel**

Chemical element	C	Mn	Si	P	Al	Fe
Weight percentage	0.20	2.20	0.53	0.0094	0.89	Balanced

2.2. Fatigue Tests

Low-cycle fatigue tests were performed on a MTS servo-hydraulic machine under the total axial strain control $\Delta\varepsilon_t$ ranging from 0.6% to 1.4%. A push-pull mode ($R_\varepsilon = -1$), a triangular waveform and a constant strain rate of $2.10^{-3} \cdot s^{-1}$ were employed.

Flat specimens, with a 12 mm gauge length and 6 mm width, were machined within the rolling direction of the steel sheet. Strain was measured by means of an extensometer of 8 mm gauge length.

The surfaces of the specimens were finely polished before testing. The fatigue life was defined as the number of cycles leading to a drop of 25% of the tensile stress taking as a reference the mid-life pseudo stabilized hysteresis loop. The plastic strain was obtained by hysteresis curves analysis.

2.3. Standard Microstructure Investigation

The microstructure of the TRIP steel and its evolution within mechanical straining have been characterised by means of light optical microscopy (LOM) and scanning electron microscopy (SEM). Here, a FEI Quanta 400 SEM has been used for fractography analysis and standard surface analysis.

Regarding the microstructure identification, etchants which are recognised to be suitable for TRIP steel have been used [17]. The selected etchants were Lepera and sodium metabisulfite + Nital cumulative etching.

For deep microstructural analyses, samples were polished with colloidal suspension. Electron backscattering diffraction analyses were carried out on a JEOL 7800F electron microscope fitted with an Oxford Instruments Aztec EDS/EBSD System.

The EBSD patterns were acquired with a Nordlys Max II detector, with a 2×2 binning corresponding to a resolution of 320×240 pixels. The parameters used for data collection were selected in order to ensure a good compromise between angular resolution and acquisition time. Then, a step size of 70 nm was chosen according to the optimisation method proposed by Chen *et al.* [18]. In a same way, by choosing the highest possible image resolutions for pattern processing and by optimising the Hough transform parameters, an angular resolution of 0.16° has been measured. The data were post-processed using both Oxford Instruments Channel 5 and TSL OIM7 commercial software.

3. Results and Discussion

3.1. Initial Microstructure Identification

The steel microstructure, as revealed by Lepera etching and analysed by LOM, is reported in Fig. 2, *a*. In order to obtain more details regarding the morphology of the encountered constituents, standard SEM analysis, using a FEI Quanta 400 W-SEM, was carried out after cumulative etching. The resulted microstructure observation is reported in Fig. 2, *b*.

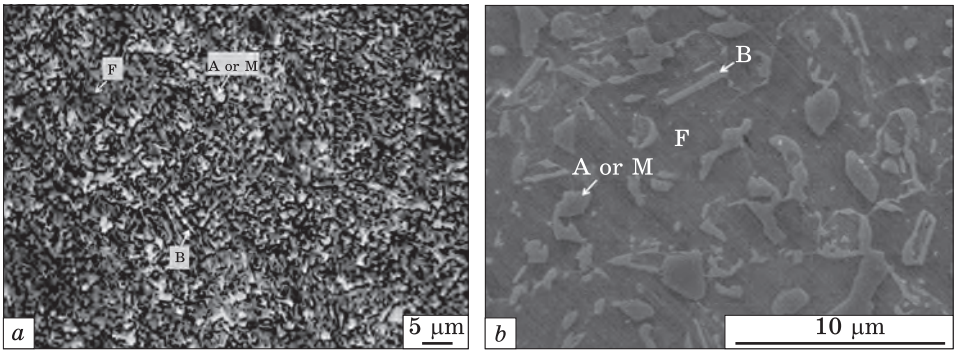

Fig. 2. Micrographs of TRIP 800 steel, LOM, Lepera etchant (*a*) and SEM micrograph of TRIP 800 steel, cumulative etching (*b*)

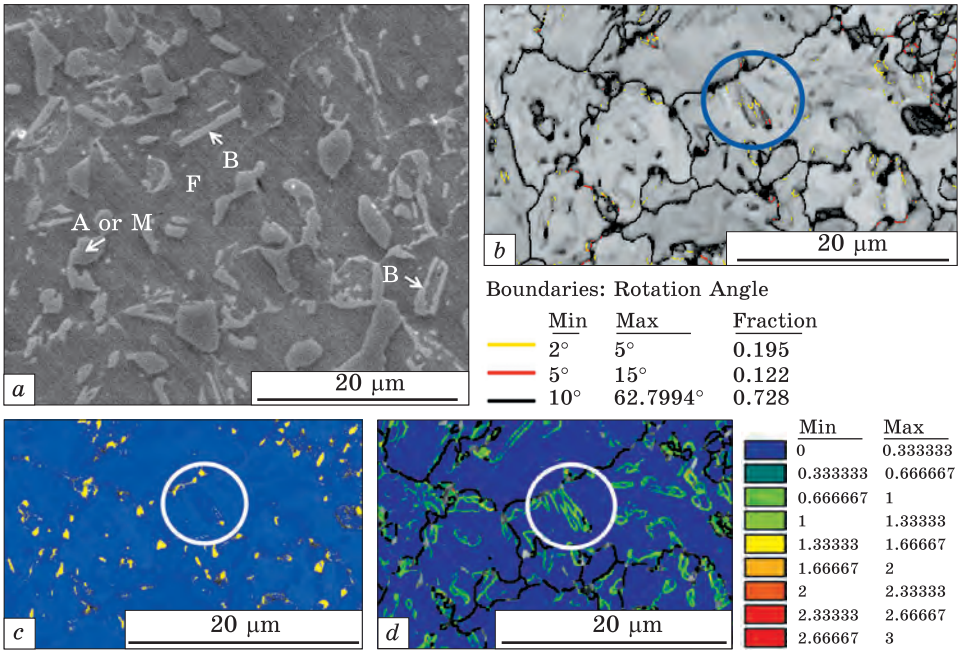

Fig. 3. Images of (*a*) bainite microstructure, (*b*) grain-boundary map, (*c*) phase map (blue — b.c.c. ferrite, yellow — f.c.c. austenite), and (*d*) KAM mapping

In those observations the ferrite matrix (F) appears in dark brown colour, retained austenite (A) appears in white and bainite (B) in lamellar structure according to Girault *et al.* [17, 19]. Note that the brightest phases may correspond to A or M (austenite or martensite), since constituent-phases do not always show a unique appearance compared to correlation among the local carbon content. Therefore, the carbon-rich phases austenite and martensite may both appear in white, whereas bainite may appear brownish to white depending on its residual carbon content and dislocation density [20].

Although LOM and SEM are unable to distinguish clearly austenite from martensite, SEM can give some indication regarding the bainite grain shape. The separation between bainitic ferrite and ferrite requires advanced data analysis as there is no clear crystallographic differences when comparing these both b.c.c. related constituents.

Then, in order to reach a much clearer distinction between these phases with good-accurate scale, an EBSD analysis and its post-processing were performed on the as-received samples. Here, Fig. 3 shows image quality (Fig. 3, *b*), phase identification (Fig. 3, *c*), and Kernel average misorientation (KAM) mapping (Fig. 3, *d*). As mentioned previously, the distinction between ferrite and bainitic ferrite remains unclear if only the crystallographic parameters are taken into consideration. Nevertheless, when considering an area that exhibits the shape of a bainite grain (as surrounded by a circle), a variation in term of disorientation is observed and might be induced by the presence of geometrically necessary dislocations (GND), which appears during the austenite to bainite transformation, as described by Zaefferer *et al.* [20].

3.2. Cyclic Strain Accommodation

The evolution of the stress amplitude with the number of cycles of the TRIP 800 steel is reported, respectively, in Figs. 4, *a* and *b*. It is characterised by a moderate hardening stage occurring during the first 10 cycles followed by a slight softening. Figure 4, *b* suggests that TRIP soften continuously during fatigue under total strain control. At first, a pronounced primary softening is observed for a period of 10% of the fatigue life. For the remaining part of the life, TRIP 800 gently softens. This observation is comparable with that of TRIP steels analysed in the literature [13, 15].

3.3. Fractography and Surface Analysis

SEM observations of the external surface of the samples after fatigue tests highlight the effect of cyclic loading. Slip marks of the specimens fatigued at $\Delta\varepsilon_t = 0.6\%$ and $\Delta\varepsilon_t = 0.8\%$ up to failure are reported in Fig. 5. The external surfaces are covered by extrusions and along some

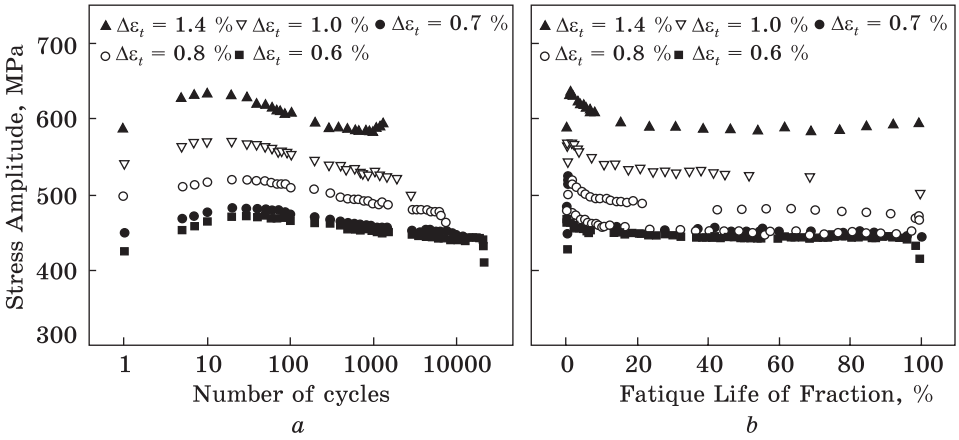

Fig. 4. Stress amplitude *vs.* number of cycles (*a*) and fatigue life fraction (*b*) for the TRIP 800 steel at a room temperature and a strain rate of $2 \cdot 10^{-2}$ s^{-1}

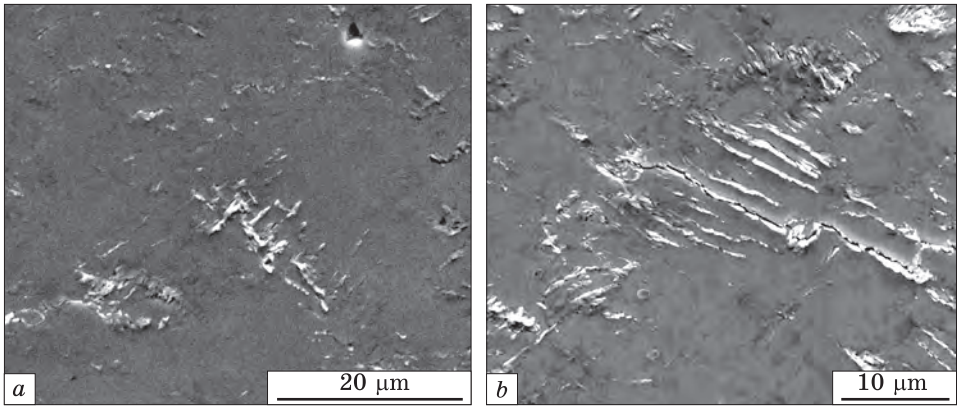

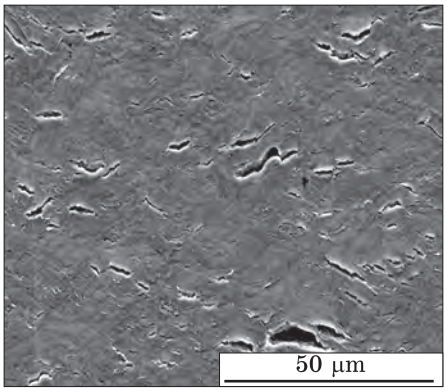

Fig. 5. SEM observations of the external surfaces of the TRIP 800 steel after fatigue at Δε$_t$ = 0.6% (*a*) and Δε$_t$ = 0.8% (*b*)

Fig. 6. SEM observations of the external surfaces of TRIP 800 steel after fatigue at Δε$_t$ = 1.4% pointing out short and long micro-cracks

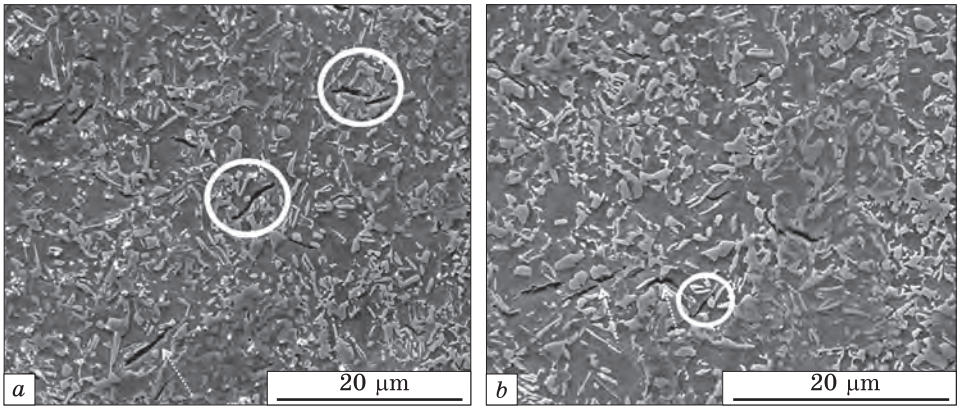

Fig. 7. SEM surface observation of the external surface of the sample fatigued at $\Delta\varepsilon_t = 1.4\%$ after etching

of them micro-cracks propagated. The extrusions density increases as the strain range increases but remains aligned only one direction.

For the sample deformed at the higher strain level, cracks were oriented along two directions, appeared to be more open and were either short or long, as reported in Fig. 6. Two populations of cracks are presented on the flat area of the specimen: short and long. This may indicate that cracks originate from different phases. The most open cracks may initiate in soft phase, allowing the crack to open.

In order to evidence the location of those cracks within the TRIP steel microstructure, the surface of the sample after fatigue testing has been etched. The resulting SEM micrographs are reported in Fig. 7. As observed, micro-cracks are located in the ferritic matrix and at the interface with the M/A and bainite constituents, rather along the bainite.

The correlation between matrix and other constituents is point of interest, because cracks propagate mostly in ferrite, along other phases. The decohesion, which takes place and leads to more opened cracks, might be related to the different level of hardness between the soft ferritic constituent and the much harder surrounding constituents. Paying deeper attention suggests that cracks seem to initiate from the hard M/A islands and propagate further into the ferrite surrounding constituents (Fig. 8).

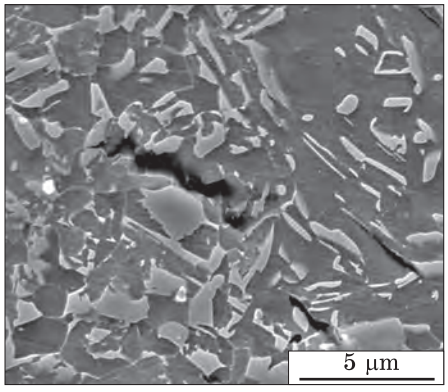

Fig. 8. Surface observation showing the crack initiation within the 'hard' constituents

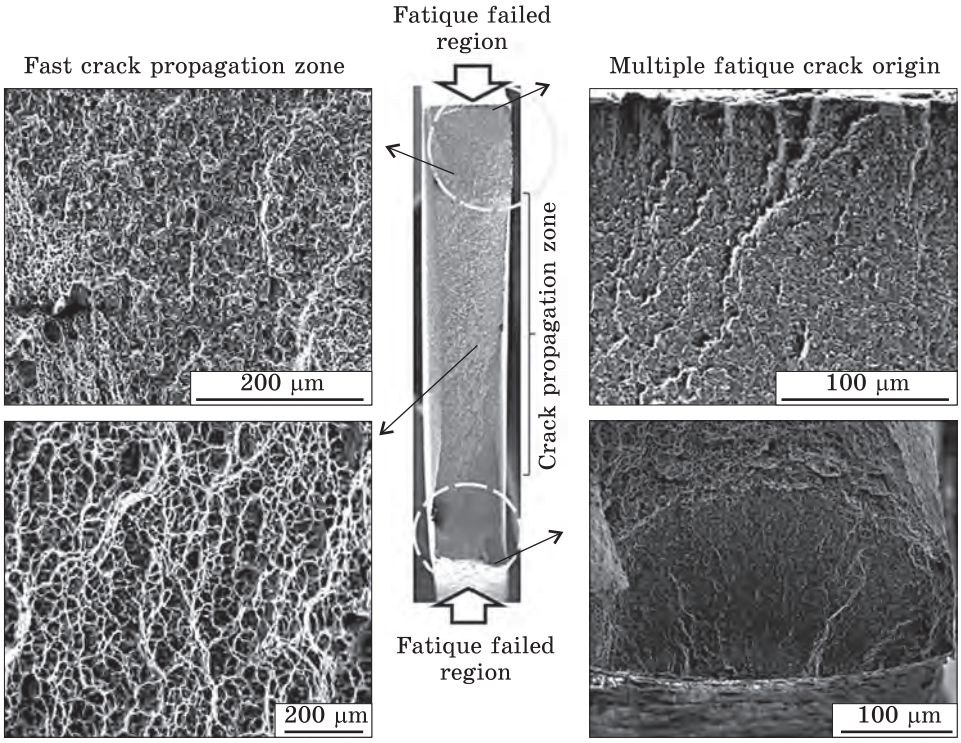

Fig. 9. SEM micrographs showing low- and high-magnification images of the fracture surface of the sample fatigued at $\Delta\varepsilon_t = 1.4\%$

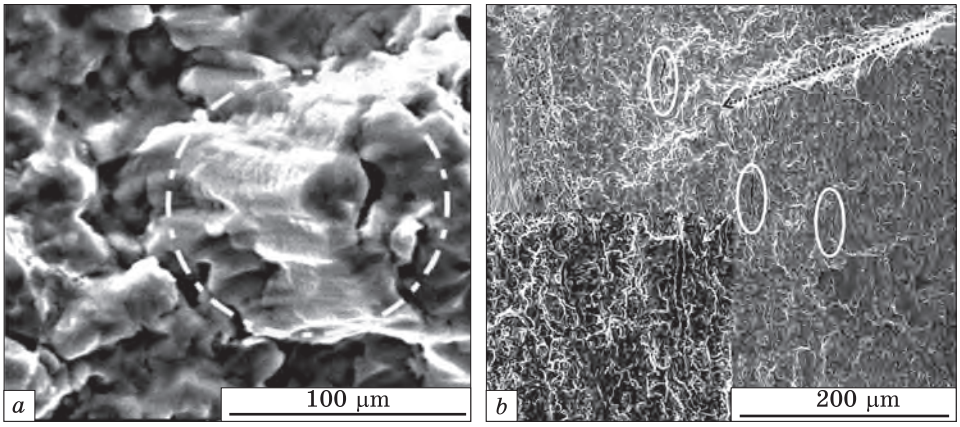

Fig. 10. Fracture surface of the specimen fatigued at $\Delta\varepsilon_t = 0.6\%$ (*a*) and $\Delta\varepsilon_t = 0.7\%$ (*b*), where fatigue striations (*a*) and secondary cracks (*b*) are observed

Those observations show similarities with literature findings [13, 16]. No crack initiation was detected neither on pores and precipitates in the low-strained (0.6%) nor on the high-strained (1.4%) samples.

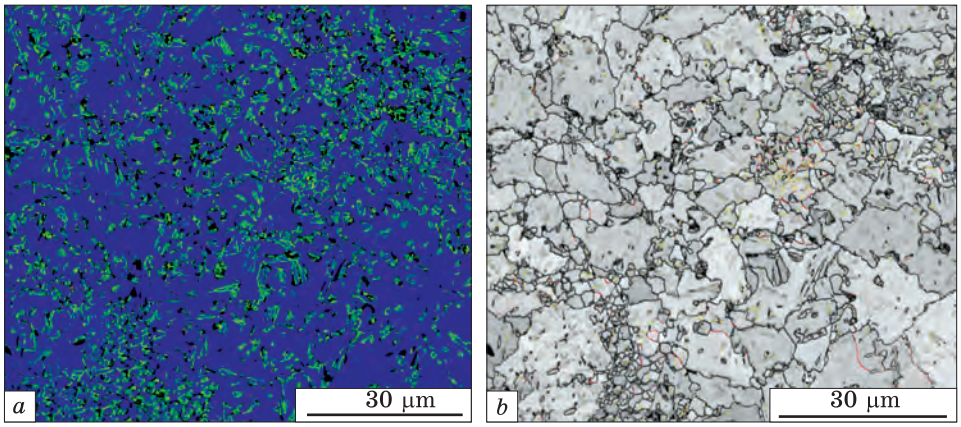

Fig. 11. KAM (*a*) and high resolution IQ + LAGB (*b*) maps of the as-received material. KAM maps after fatigue at $\Delta\varepsilon_t$ = 0.6% (*c*) and $\Delta\varepsilon_t$ = 1.2% (*d*)

The study of the fractured surfaces is reported in Figs. 9 and 10. The fracture surfaces comprise different zones corresponding to either crack propagation by fatigue or to final and monotonic fracture. The latter occupies the central part of the specimen and was all the wider as the strain range was high. The borders of the fracture surface exhibited plastic deformation associated with necking. The ductile feature of this fracture was confirmed by the presence of dimples imaged at higher magnification. The fatigue crack propagation zones were, in general, near the edges of the specimen and appeared flat.

Fatigue fracture surface is usually identifiable by the presence of striations. For this material and the experimental conditions, striations were hardly observed due to fretting effect of the surfaces (Fig. 10, *a*). Many secondary cracks were also observed (Fig. 10, *b*).

3.4. Advanced Microstructure Analysis

In order to evaluate the microstructure evolution of the TRIP 800 steel when the latter was submitted to cyclic loading, SEM-EBSD investigation has been carried out. As the local misorientation, evolution studied by KAM gives some indications on the variation of GND density and hence the local strain, this criterion was selected. Note that in the present case, due to the complex microstructure, the results obtained with this parameter are only qualitative. Indeed, it is known that for the as received materials for example, the GND density is higher in the bainitic ferrite regions [20] than in the other ones. In addition, EBSD post-processing has been performed on non-deformed (as received) and strained samples in order to highlight stress-induced microstructural changes.

As expected, and reported in the Fig. 11, *a*, the KAM distribution of as-received material appears as rather not homogeneous at the mesoscopic scale. This clearly corresponds to the presence of bainitic ferrite regions for which the measured misorientation is higher due to the presence of GND. This can be more clearly seen when the low-angle grain boundaries (LAGB) are plotted within the global microstructure, see the red coloured line in Fig. 11, *b*. Additional EBSD data processing has shown that, for one piece of material taken from one spot to another one in the plate, the microstructure was very inhomogeneous. Indeed, KAM map has pointed out a higher density of misoriented areas suggesting that the material was more or less deformed and/or transformed from one specimen to another one.

The KAM maps obtained on fatigued samples clearly point out an impact of the accumulated cyclic strain on the microstructure. Figures 11, *a*, *d* are the KAM maps of the same specimen respectively before and after fatigue at $\Delta\varepsilon_t = 1.2\%$. Strain accumulation is clearly seen through the spatial distribution of areas with larger KAM values. This can be explained by the fact that a very high plastic strain since the beginning of cycling transforms the metastable austenite into martensite, which tends to localize the deformation.

According to the literature [21], high martensite volume fractions lead to higher local stresses. A strong deviation of stress distribution within the grain gives a heterogeneous strain distribution within the matrix material. Thereby, the literature [22, 23] draws our attention on the heterogeneity of strain between constituents. Maximum of strain gradient is at the interface between the ferritic matrix and the second phase(s). The heterogeneity correlates with an increase of local strain in the grain.

These observations may explain the presence of two different cracks populations observed previously.

4. Conclusions

The low cycle fatigue behaviour of the TRIP 800 steel has been investigated at room temperature under total strain control and the evolution of the microstructure with cycling studied by SEM-EBSD.

The following conclusions can be drawn:

(i) the material exhibits an appreciable cyclic softening during the first percentages of the fatigue life;

(ii) short cracks are observed in the ferritic matrix and were often associated with interfaces between ferrite matrix and hard phases;

(iii) EBSD data processing leading to KAM criterion is relevant for characterization of the fatigued microstructure;

(iv) KAM criterion points out the inhomogeneity of the microstructure inside the plate from which the fatigue specimens were extracted;

(v) KAM criterion points out localisation of deformation after fatigue.

REFERENCES

1. Z.A. Duryahina, A.K. Borysyuk, S.A. Bespalov, and V.Y. Pidkova, *Mater. Sci.*, **48**, No. 3: 364 (2012). https://doi.org/10.1007/s11003-012-9514-x
2. Z.A. Duryagina, S.A. Bespalov, A.K. Borysyuk, and V.Ya. Pidkova, *Metallofiz. Noveishie Tekhnol.*, **33**, No. 5: 615 (2011).
3. N. Fonstein, *Advanced High Strength Sheet Steels* (Cham: Springer: 2015). https://doi.org/10.1007/978-3-319-19165-2
4. J.J. Roa, I. Sapezanskaia, G. Fargas, R. Kouitat, A. Redjaïmia, and A. Mateo, *Mater. Sci. Eng. A*, **713**: 287 (2018). https://doi.org/10.1016/j.msea.2017.12.047
5. J. Van Slycken, J. Bouquerel, P. Verleysen, K. Verbeken, J. Degrieck, and Y. Houbaert, *Mater. Sci. Forum*, **638–642**: 3585 (2010). https://doi.org/10.4028/www.scientific.net/MSF.638-642.3585
6. P.J. Jacques, Q. Furnemont, S. Godet, T. Pardoen, K.T. Conlon, and F. Delannay, *Phil. Mag.*, **86**, No. 16: 2371 (2006). https://doi.org/10.1080/14786430500529359
7. H. Mousalou, A. Noori Teymorlu, N. Parvini Ahmadi, and S. Yazdani, *Int. J. Iron & Steel Society of Iran*, **9**, No. 1: 11 (2012).
8. I.-J. Park, S.-T. Kim, I.-S. Lee, Y.-S. Park, and M.B. Moon, *Mater. Trans.*, **50**, No. 6: 1440 (2009). https://doi.org/10.2320/matertrans.mra2008252
9. S. Chatterjee, *Transformations in TRIP-Assisted Steels: Microstructure and Properties* (Darwin College: University of Cambridge: 2006).
10. O. Hesse, J. Merker, M. Brykov and V. Efremenko, *Tribologie und Schmierungstechnik*, **60**, No. 6: 37 (2013) (in German).
11. P.I. Christodoulou, A.T. Kermanidis, and D. Krizan, *Int. J. Fatigue*, **91**, Part 1: 220 (2016). https://doi.org/10.1016/j.ijfatigue.2016.06.004
12. L.T. Robertson, T.B. Hilditch, and P.D. Hodgson, *Int. J. Fatigue*, **30**, No. 4: 587 (2008). https://doi.org/10.1016/j.ijfatigue.2007.06.002

13. T. Hilditch, H. Beladi, P. Hodgson, and N. Stanford, *Mater. Sci. Eng. A*, **534**: 288 (2012).
https://doi.org/10.1016/j.msea.2011.11.071
14. A.L. Ly and K.O. Findley, *Int. J. Fatigue*, **87**: 225 (2016).
https://doi.org/10.1016/j.ijfatigue.2016.02.004
15. M. Benedetti, V. Fontanari, M. Barozzi, D. Gabellone, M.M. Tedesco, and S. Plano, *Fatigue Fract. Engng. Mater. Struct.*, **40**, No. 9: 1459 (2017).
https://doi.org/10.1111/ffe.12589
16. M. Abareshi and E. Emadoddin, *Mater. Des.*, **32**, No. 10: 5099 (2011).
https://doi.org/10.1016/J.MATDES.2011.06.018
17. E. Girault, P. Jacques, P. Harlet, K. Mols, J. Van Humbeeck, E. Aernoudt, and F. Delannay, *Mater. Charact.*, **40**, No. 2: 111 (1998).
https://doi.org/10.1016/S1044-5803(97)00154-X
18. Y. Chen, J. Hjelen, S. S. Gireesh, and H. J. Roven, *J. Microsc.*, **245**, No. 2: 111 (2012).
https://doi.org/10.1111/j.1365-2818.2011.03551.x
19. E. Girault, A. Mertens, P.J. Jacques, Y. Houbaert, B. Verlinden, and J. Van Humbeeck, *Scr. Mater.*, **44**, No. 6: 885 (2001).
https://doi.org/10.1016/S1359-6462(00)00697-7
20. S. Zaefferer, P. Romano, and F. Friedel, *J. Microsc.*, **230**, No. 3: 499 (2008).
https://doi.org/10.1111/j.1365-2818.2008.02010.x
21. H. Quade, U. Prahl, and W. Bleck, *Chemicke Listy*, **105**: s705 (2011).
22. Q. Furnémont, M. Kempf, P.J. Jacques, M. Göken, and F. Delannay, *Mater. Sci. Eng. A*, **328**, Nos. 1–2: 26 (2002).
https://doi.org/10.1016/S0921-5093(01)01689-6
23. R.H. Petrov, J. Bouquerel, K. Verbeken, L.A.I. Kestens, P. Verleysen, and Y. Houbaert, *Mater. Sci. Forum*, **638–642**: 3447 (2010).
https://doi.org/10.4028/www.scientific.net/MSF.638-642.3447

Received July 15, 2019;
in final version, November 04, 2019

З.М. Рикавець[1], *Ж. Букерель*[2], *Ж.-Б. Воґьот*[2], *З.А. Дурягіна*[1,3],
В.В. Кулик[1], *Т.Л. Тепла*[1], *Л.І. Богун*[1], *Т.М. Ковбасюк*[1]

[1] Національний університет «Львівська політехніка»,
вул. С. Бандери 12, 79013 Львів, Україна
[2] Університет науки та технології Лілль I,
відділення матеріалів і перетворень,
Наукове містечко, 59650 Вільнев-д'Аск, Франція
[3] Люблінський католицький університет Яна Павла II,
ал. Рацлавіцкє, 14, 20-950 Люблін, Польща

ДОСЛІДЖЕННЯ МІКРОСТРУКТУРИ ТА ВЛАСТИВОСТЕЙ КРИЦІ TRIP 800, СХИЛЬНОЇ ДО МАЛОЦИКЛОВОЇ ВТОМИ

Низьколеґовані TRIP-криці добре відомі з початку XXI століття та використовуються в автомобілебудуванні задля забезпечення пасивної безпеки. Хоча їхню поведінку цілком досліджено за монотонного навантаження, проте недостатньо вивчено за циклічного навантаження. Дана робота детально описує гетерогенну еволюцію мікроструктури високоміцної криці (TRIP 800) за умов малоциклової втоми. На підставі розширених досліджень (оптичною й електронною мікроскопією, дифракцією зворотнього розсіяння електронів) запропоновано реко-

мендації щодо впливу фазового складу на механічні властивості та процеси зародження тріщин. Виявлено осередки переважного зародження тріщини, спричинені втомою, й оцінено повноту фазового перетворення за рахунок індукованої пластичности.

Ключові слова: малоциклова втома, мікроструктура, фрактографія, дифракція відбитих електронів.

З.М. Рыкавець[1], *Ж. Букэрель*[2], *Ж.-Б. Вогёт*[2], *З.А. Дурягина*[1,3], *В.В. Кулык*[1], *Т.Л. Тэпла*[1], *Л.И. Богун*[1], *Т.М. Ковбасюк*[1]

[1] Национальный университет «Львовская политехника», ул. С. Бандэры, 12, 79013 Львов, Украина

[2] Университет науки и технологии Лилль I, отдел материалов и преобразований, Научный город, 59650 Вильнев-д'Аск, Франция

[3] Люблинский католический университет Яна Павла II, ал. Рацлавицке, 14, 20-950 Люблин, Польша

ИССЛЕДОВАНИЕ МИКРОСТРУКТУРЫ И СВОЙСТВ СТАЛИ TRIP 800, ПОДВЕРЖЕННОЙ МАЛОЦИКЛОВОЙ УСТАЛОСТИ

Низколегированные TRIP стали хорошо известны с начала XXI века и используются в автомобилестроении для обеспечения пассивной безопасности. Хотя их поведение вполне исследовано при монотонной нагрузке, однако недостаточно изучено при циклической нагрузке. Данная работа подробно описывает гетерогенную эволюцию микроструктуры высокопрочной стали (TRIP 800) в условиях малоцикловой усталости. На основании расширенных исследований (оптической и электронной микроскопией, дифракцией обратного рассеяния электронов) предложены рекомендации относительно влияния фазового состава на механические свойства и процессы зарождения трещин. Обнаружены очаги предпочтительного зарождения трещины, что вызвано усталостью, и оценена полнота фазового превращения за счёт индуцированной пластичности.

Ключевые слова: малоцикловая усталость, микроструктура, фрактография, дифракция отражённых электронов.